Short communication

A newly-developed effective direct current assisted sintering technique for electrolyte film densification of anode-supported solid oxide fuel cells

Yajie Liu, Xiaoming Hao, Zhenhua Wang *, Jiawei Wang, Jinshuo Qiao, Yiming Yan, Kening Sun *

School of Chemical Engineering and Environment, Beijing Institute of Technology, Beijing 100081, PR China

HIGHLIGHTS

► A DC assisted sintering technique was developed for electrolyte film densification.
► A fully dense YSZ film was obtained with a short sintering time and low temperature.
► The grain growth was inhibited during the DC assisted sintering process.
► The perfect cell performance ascribed to the fine YSZ film and good anode structure.
► This technique may provide a promising way to fabricate nano-structured cells.

ARTICLE INFO

ABSTRACT

In order to lower the sintering temperature and shorten firing time, a novel, effective and facile technique has been developed for sintering Yttria-stabilized zirconia (YSZ) electrolyte thin film. Herein this technique, which employs a weak direct current (DC), is used for the first time in the manufacture of the anode-supported solid oxide fuel cell (SOFC). A single cell is directly assembled using a pre-sintered anode/electrolyte and screen printed cathode and subsequently sintered under electric assistance from room temperature to 800 °C at a heating rate of 5 °C min^{-1}. A fully dense YSZ electrolyte film can be observed by scanning electron microscopy (SEM) and the open circuit voltages (OCVs) are in accordance with theoretical values, confirming that the cell possesses a dense YSZ film. Using hydrogen fuel, the maximum power density of this cell was 0.8, 1.1 and 1.4 W cm^{-2} at 650, 700 and 750 °C, respectively. We believe this DC assisted sintering technique (DC-AST) may not only reduce the cost, but also maintain the anode nanostructure, thus offering a potentially useful manufacturing technique for SOFCs.

1. Introduction

In the context of highly efficient and pollution-free energy sources, solid oxide fuel cells (SOFCs) have been intensively studied over the several decades. SOFCs, applying solid oxides as an electrolyte, are electrochemical devices that transform the chemical energy of fuels (hydrogen, natural gas, etc.) directly to electrical energy. SOFCs possess some unique advantages over the traditional power generation technologies, including inherently high efficiency, low greenhouse emissions and fuel flexibility [1–3]. Because of their excellent high temperature ionic conductivity and mechanical strength, zirconia-based electrolytes, such as YSZ, have long been recognized as one of the most promising candidates for commercial application in SOFCs [4,5]. However, in conventional sintering (ordinary sintering, hot pressing, sinter forging and hot isostatic pressing), high temperatures of 1400 °C or more and sintering times of several hours are required to produce a dense 8 mol % Y_2O_3 in ZrO_2 (8YSZ) film. Such high temperature and time-intensive processes are not only expensive in terms of energy and equipment, but they can also change or destroy the anode microstructure, thus retarding the overall performance of SOFCs.

To overcome the above mentioned problem, considerable effort has been made to reduce the co-sintering temperature. One approach consists of the addition of sintering aids. For example Batista and Muccillo [6], reported that a small amount of (up to 1.0 mol%) of NiO was available to improve the sinterability of YSZ at 1350 °C over 0.5 h. However, many sintering aids could lower the conductivity and the mechanical strength of electrolyte. Thus increased research has focused on nonconventional sintering technologies. Such techniques, including pulsed electric current sintering (PECS) [7], microwave (MW) [8] and flash-sintering (FS) provide alternatives to the densification of YSZ ceramics. In particular, the non-conventional flash sintering technique has been

applied to several oxides including Yttria doped Zirconia (8YSZ and 3YSZ), Gadolinia doped Ceria (GDC) and Cobalt Manganese Oxide (Co_2MnO_4) [9–11]. It has been demonstrated that 8YSZ can be sintered in several seconds at 750 °C to full density by applying a DC electrical field of 150 V cm^{-1} [12]. However, very few nonconventional sintering techniques have been applied to solid oxide fuel cells, in particular the sintering of the anode-supported electrolyte films.

In the present work, a newly-developed and facile sintering technique (DC-AST) was developed to sinter 8YSZ electrolyte film. A resulting dense film was obtained using a shorter sintering time and lower sintering temperature. Observations from SEM imaging suggest a possible grain growth process in DC-AST. Also with regard to the electrochemical performance, the discharge and impedance tests further demonstrate the application potential of our sintering technique in SOFCs manufacture.

2. Materials and methods

Eight mol% Y_2O_3 in ZrO_2 (8YSZ) (Tosoh®, Japan) was used as the electrolyte; a mixture of NiO (Tosoh®, Japan), 8YSZ and pore-former was used for the anode-support. The anode and electrolyte were prepared by tape-casting technology [13,14]. A green tape of anode/electrolyte was cut into discs with a diameter of 2 cm. The half-cells were pre-sintered on sinter support plates (electrolyte on top) for 2 h at 1300 °C to remove any organic materials and obtain suitable mechanical strength. After pre-sintering, an electrolyte with a porosity of 40–50 vol.% was observed by a scanning electron micrograph (SEM). The $La_{0.8}Sr_{0.2}MnO_x$ (LSM, Praxair, Inc., USA) cathode was prepared through screen-printing. An illustration of the DC-AST device is shown in Fig. 1. After pre-sintering, the cell was assembled on an alumina tube and sealed with silver electric adhesive. In order for the electrolyte film to apply a constant DC electric voltage, one Pt wire was adhered to the cathode using silver paste and another connected to the silver electric adhesive. Thus, a field can be formed in the electrolyte layer and current radiates from the central part of electrolyte to the edge when a certain voltage is applied (see Fig. 1 inset). Afterwards the cell was placed in the tube furnace, and temperature increased at rate of 5 °C min^{-1} from room temperature to 800 °C, while a constant voltage (16 V) was supplied. The values of the current and time were measured by a Keithley2400 and recorded. When the temperature reached 800 °C, DC-AST sintering was terminated. Once complete, the cell was tested by an Arbin Instruments (Eload, Arbin Instrument, College Station, U.S.A.). The performance was measured with 75

standard cubic centimetres per minute (sccm^{-1}) of dry H_2 fuel at 750, 700, 650 °C. Electrochemical impedance spectra (EIS) were collected using M2273 advanced electrochemical system (Parstat) over a frequency range of 100 −100 MHz at open circuit conditions. Scanning electron microscopy (FEI Quanta 250) was used to observe the cell microstructure.

3. Results and discussion

3.1. The DC assisted sintering process

The relationship between current, power and temperature during the DC assisted sintering process is shown in Fig. 2. The current was proportional to the rise of temperature during the whole process, with the ultimate current value was of 45 mA. It has previously been reported that a bone-shape 8YSZ lump could be sintered to full density in a few seconds at 750 °C by applying a DC electrical field of 150 V cm^{-1} (FS) [12]. However, this sintering technique often operates at a high voltage and large power dissipation, which produces instantaneous shrinkage and results in uncontrollable collapse. Compared with FS, a smooth and constantly increasing weak current can play a critical different role in electrolyte film densification. It was considered that the densification of electrolyte thin film should be a gradually developing process, which occurred in the current rising procedure (the heating rate is 5 °C min^{-1} in this process). The ease of controlling the direct current assisted sintering technique (DC-AST) was thus more appropriate for electrolyte film sintering with the advantage of avoiding uncontrollable collapse.

3.2. SEM micrographs and grain growth simulation

The SEM micrographs of samples before and after DC assisted sintering are shown in Fig. 3. From Fig. 3(b) and (d), we can see that a dense film of YSZ electrolyte was achieved in an extremely short time by DC assisted sintering. Furthermore, it can be noted from Fig. 3(d) that a large quantity of nano-particles appeared around the micro-particles, which implies that the grain growth was suppressed by the weak direct current in the DC-AST sintering process [15,16]. The cross-sectional image of fully dense YSZ thin film (thickness of ∼10.4 μm) and uniform functional layer (thickness of ∼30 μm) is shown in Fig. 3(c). The grain sizes were measured by SEM and appropriate software using the intercept method. Fig. 4 shows the comparison of DC assisted sintering and conventional sintering samples giving the average sizes of 440 nm and 4.06 μm,
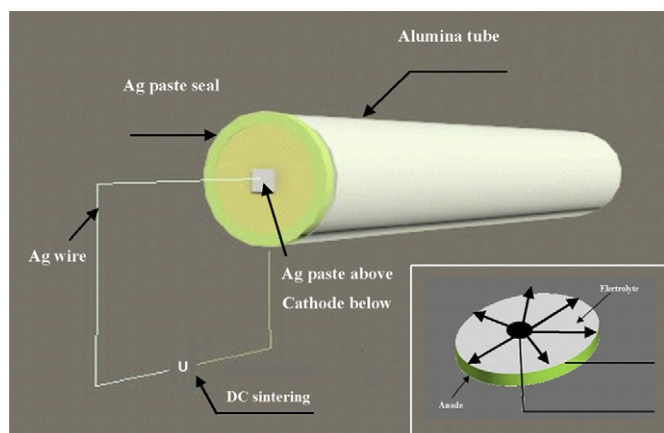

Fig. 1. Illustration of DC assisted sintering device. The current radiates from the central part of electrolyte to the edge.
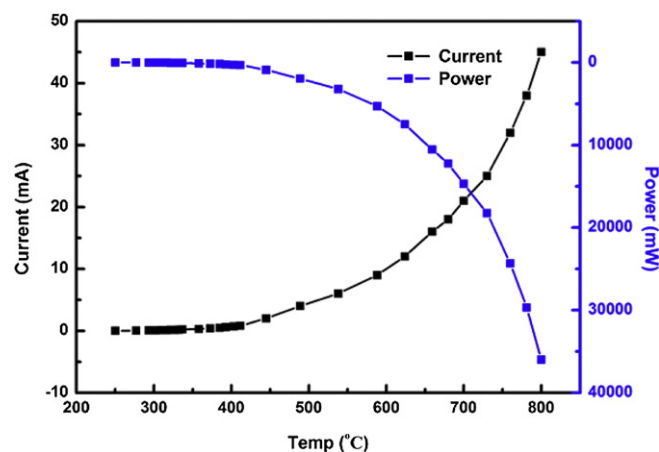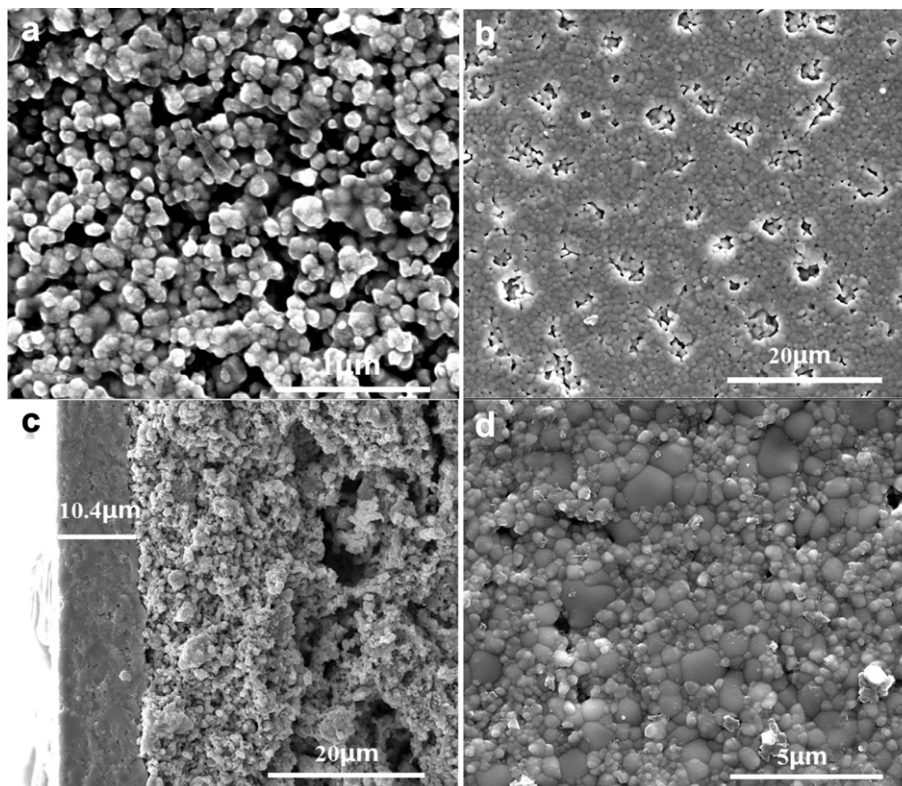

Fig. 2. I/T and P/T curves during DC assisted sintering process with a voltage of 16 V.

Fig. 3. Micro-scale SEM images of SOFC (a) the electrolyte surface of green tape; (b) the electrolyte surface after pre-sintering; (c) cross-section after DC assisted sintering; (d) dense electrolyte surface after DC assisted sintering. (For interpretation of the references to colour in this figure legend, the reader is referred to the web version of this article.)

respectively. It was seen that DC assisted sintering results in a finer microstructure than conventional sintering which is most likely due to the lack of high temperature and shorter sintering time.

Studies by Huang [17], Han [18] and Chaim [19] on grain growth without using a field, indicated that the mechanism of DC-AST, in terms of retardation of grain growth, could be partly explained by two mechanisms: (1) Joule heating at the grain boundaries [20], (2) a reduction in the grain boundary energy γ_{gb} (the driving force) by the interaction of the field with the space charge [21]. Herein we suggest that the sintering at inter-particle boundary might be enhanced by the effect of the space charge driven by a weak direct current, while the short time of the sintering process inhibits grain growth.

The grain growth process was simulated in Fig. 5. Here the electrolyte film supported by the anode was sintered through a two step process, including pre-sintering and DC-AST sintering. For these steps, differing from conventional sintering, the grain growth during the microstructure development was investigated to understand the sintering process better. The tape-casted green tape was pre-sintered at 1300 °C as the first step. Within the 700–1100 °C range, any organic material was removed and the necks at particle junctions grew by surface diffusion as well as by grain-boundary diffusion. At reaching 1300 °C, the surface diffusion-induced neck growth as domination was further developed, and lead to the granular aggregate. However, grain-boundary diffusion growth resulted in physical shrinkage (densification) of the aggregate, whereas surface diffusion-induced neck growth would not [22]. When the first step was finished, the electrolyte contained 40–50 vol.% porosity as viewed by SEM in Fig. 3(b). In the DC assisted sintering, because of the effect of the space charge in
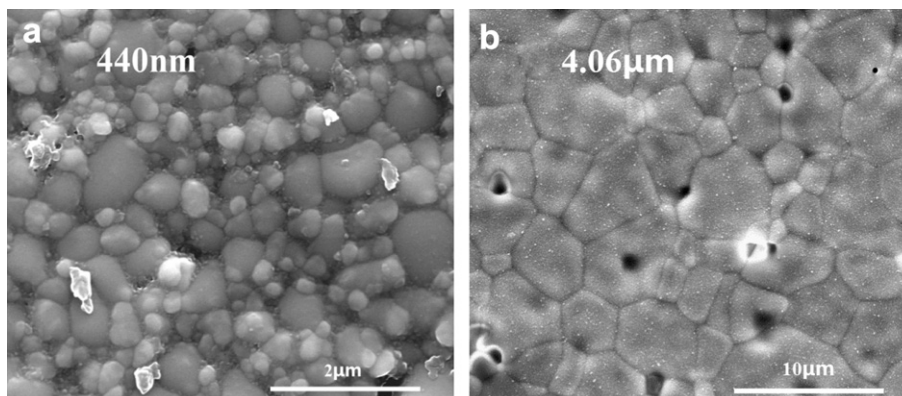
Fig. 4. Grain size with (a) DC assisted sintering and (b) conventional sintering.
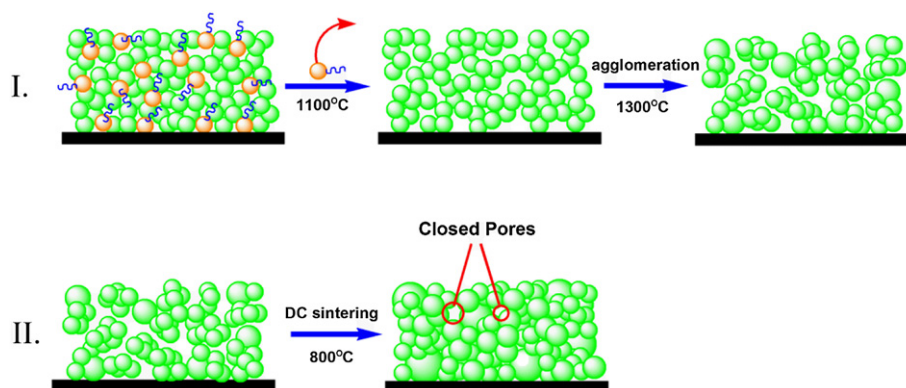
Fig. 5. Simulation of the grain growth in the whole sintering process (the red balls stand for organic material, and the green balls stand for YSZ grains). (For interpretation of the references to colour in this figure legend, the reader is referred to the web version of this article.)

the grain-boundary (between the space of two or more grains), the grain-boundary diffusion may therefore be enhanced in this process. Moreover, grain growth was suppressed but conversely the densification was increased. Ultimately, the pores were filled with small nano-crystals by mass diffusion in the DC assisted sintering process.

3.3. Electrochemical properties

The discharge results of cells sintered with or without DC assisted sintering are presented in Fig. 6. The OCV value gives credible evidence that the electrolyte film underwent densification after weak DC assisted sintering was applied. Comparing the OCV (0.693 V and 1.104 V), it appears that the density of electrolyte film was improved considerably after electrically assisted sintering. Due to the poorly dense electrolyte film, i.e. that obtained without DC assisted sintering, the I/V curve is observed to drop rapidly. Moreover, the maximum power density value of cell sintered without DC-AST was only 34% when compared to that of the DC-AST sintered in 750 °C.

Fig. 7(a) shows the cell voltages and power densities for a single cell with a $\sim$10.4 μm thick 8YSZ thin film after DC assisted sintering as a function of temperature. It shows that through the DC assisted sintering process the OCVs all exceed 1 V from 650 °C to 750 °C, within an acceptable range to the theoretical value. The peak power densities were 0.8, 1.1 and 1.4 W cm^{-2} at 650, 700 and 750 °C,

respectively, again better than that obtained from conventional sintering [23–28]. Herein we have ascribed the good performance to the reduction of the grain size both in the electrolyte and the anode. This nano-crystallinity may introduce a high density into the interfaces so that the conduction properties become interface-controlled [29]. Han et al. reported a higher ionic conductivity for 8YSZ electrolytes with a smaller grain size and with lower thicknesses of the intergranular regions [30]. Besides, the controlled
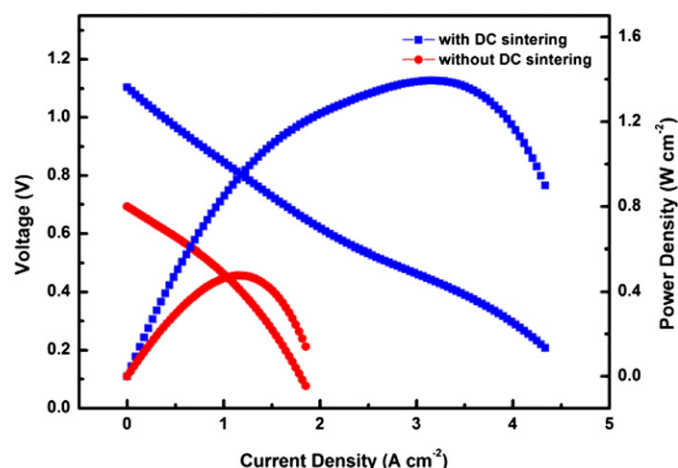
Fig. 6. I/V and I/P curves of a single cell with and without DC sintering.
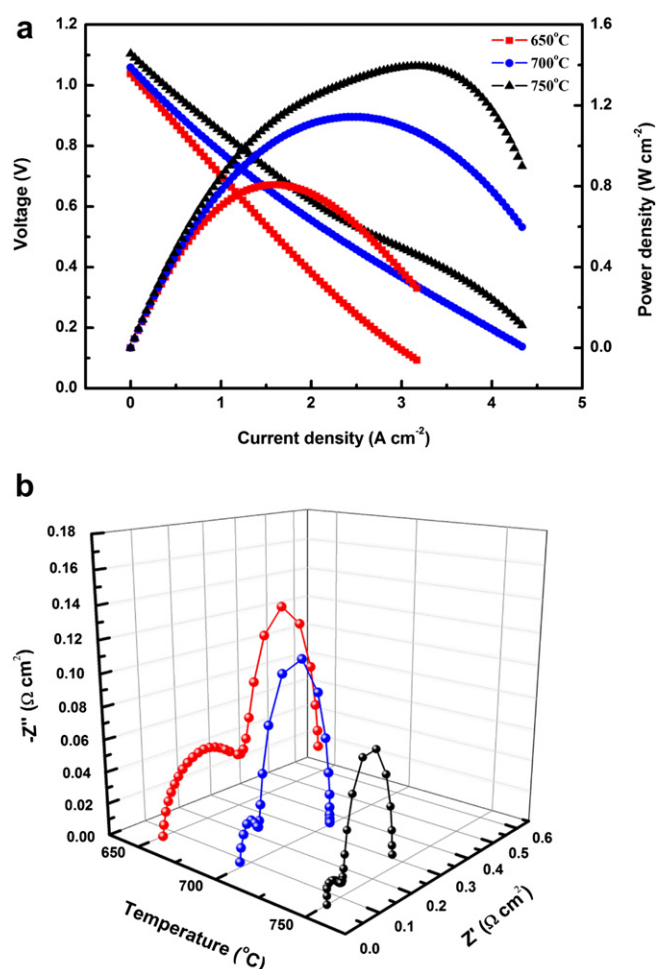
Fig. 7. (a) I/V and I/P curves of a single cell after DC assisted sintering as a function of temperature; (b) impedance spectra of the cell tested under open circuit conditions.

sintering of Ni–YSZ particles leads to smaller size, seen in Fig. 3(c), and hence a larger three phase boundary (TPB) density in a composite Ni–YSZ anode, which may also improve the performance of the cell at intermediate temperature. Fig. 7(b) shows the typical impedance spectrum of a single cell measured under open circuit conditions at different temperatures. It is evident from Fig. 7(b) that the high-frequency intercept on the real axis represents the Ohmic resistance, which is correlated to the electrolyte. Here the Ohmic resistance is only 0.061 Ω cm^2 at 750 °C, for example. The difference between the high- and low-frequency intercepts on the real axis shows the electrode polarization resistance of both the anode and cathode. The results shown in Fig. 7 indicate that the performance of the cells was limited by the overwhelming polarization resistance of the electrode, for example, which accounted for 77% of the total resistance at 750 °C. These electrochemical properties still indicated notable polarization losses, which may further increase the TPB by keeping the whole orderly nanostructure of anode. Thus, we deem that the outstanding electrochemical performance is associated with the fine grain size of the electrolyte and the good anode microstructure, resulting from the lower sintering temperature and shorter time. This novel and facile technique (DC-AST) may be of significant benefit to future SOFCs manufacture.

4. Conclusions

The sintering of the anode-supported electrolyte film of SOFC has been achieved by a novel and efficient direct current assisted sintering (DC-AST). This technique is superior to other common sintering techniques due to its relative ease in controlling the sintering process as well as avoiding the use of costly equipment. It is considered here that the application of DC may not only lead to considerable energy and time saving, but may also suppress grain growth (the average size of 440 nm) and further improve the cell performance at intermediate temperatures. Test results reveals that the OCVs of the cell with a 10 μm-thick electrolyte are all above 1 V within the temperature range from 650 °C to 750 °C, which are in good agreement with theoretical values. Furthermore, the maximum power density is 0.8, 1.1, 1.4 W cm^{-2} at 650, 700, 750 °C, respectively. These results suggest that a dense and fine YSZ layer with suitable anode microstructure can be made at lower temperature use DC-AST. The resulting fine grain size, high-conductivity electrolytes and nanostructured electrodes obtained by DC-AST may provide a possible path for further performance improvement at much lower temperatures, thus giving an opportunity to transform the way we convert and store energy.

References

[1] N.Q. Minh, J. Am. Ceram. Soc. 76 (1993) 563.
[2] S.C. Singhal, Solid State Ionics 135 (2000) 305–313.
[3] B.C.H. Steele, Solid State Ionics 134 (2000) 3.
[4] J. Li, N. Zhang, K. Sun, W. Sun, W. Li, J. Alloys Compd. 509 (2011) 5388–5393.
[5] K.J. Yoon, P. Zink, S. Gopalan, U.B. Pal, J. Power Sources 172 (2007) 39.
[6] R.M. Batista, E.N.S. Muccillo, Ceram. Int. 37 (2011) 1047–1053.
[7] Z.A. Munir, D.V. Quach, J. Am. Ceram. Soc. 94 (1) (2011) 1–19.
[8] S. Das, A.K. Mukhopadhyay, S. Datta, D. Basu, Bull. Mater. Sci. 32 (2009) 1–13.
[9] M. Cologna, B. Rashkova, R. Raj, J. Am. Ceram. Soc. 93 (11) (2010) 3556–3559.
[10] X. Hao, Y. Liu, Z. Wang, J. Qiao, K. Sun, J. Power Sources 210 (2012) 86–91.
[11] A.L.G. Prette, M. Cologna, V. Sglavo, R. Raj, J. Power Sources 196 (2011) 2061–2065.
[12] M. Cologna, A. Prette, R. Raj, J. Am. Ceram. Soc. 94 (2011) 316–319.
[13] S. Le, K. Sun, N. Zhang, X. Zhu, H. Sun, J. Power Sources 195 (2010) 2644–2648.
[14] J. Qiao, K. Sun, N. Zhang, B. Sun, J. Kong, D. Zhou, J. Power Sources 169 (2007) 253.
[15] D. Yang, R. Raj, H. Conrad, J. Am. Ceram. Soc. 93 (10) (2010) 2935–2937.
[16] S. Ghosh, A.H. Chokshi, P. Lee, R. Raj, J. Am. Ceram. Soc. 92 (8) (2009) 1856–1859.
[17] S.L. Hwang, I.W. Chen, J. Am. Ceram. Soc. 73 (1990) 3269–3277.
[18] J.H. Han, D.Y. Kim, J. Am. Ceram. Soc. 76 (1993) 538–550.
[19] R. Chaim, Mater. Sci. Eng. A 486 (2008) 439–446.
[20] S. Grasso, Y. Sakka, N. Rendtroff, C. Hu, G. Maizza, H. Borodianska, O. Vasylkiv, J. Ceram. Soc. Jpn. 119 (2) (2011) 144–146.
[21] H. Conrad, J. Am. Ceram. Soc. 94 (2011) 3641–3642.
[22] M. Cologna, R. Raj, J. Am. Ceram. Soc. 94 (2011) 391–395.
[23] X. Zhou, K. Sun, J. Gao, S. Le, N. Zhang, P. Wang, J. Power Sources 191 (2009) 528–533.
[24] M. Han, H. Yin, W. Miao, S. Zhou, Solid State Ionics 179 (2008) 1545–1548.
[25] Z. Wang, K. Sun, S. Shen, N. Zhang, J. Qiao, P. Xu, J. Membr. Sci. 320 (2008) 500–504.
[26] S. Le, K. Sun, N. Zhang, S. Shen, N. Zhang, X. Zhu, H. Sun, J. Power Sources 195 (2010) 2644–2648.
[27] Z. Wang, K. Sun, S. Shen, X. Zhou, J. Qiao, N. Zhang, J. Solid State Electrochem. 14 (2010) 637–642.
[28] Y. Zhang, X. Huang, Z. Lu, Z. Liu, X. Ge, J.X.X. Xin, X. Sha, W. Su, J. Am. Ceram. Soc. 89 (2006) 2304–2307.
[29] J. Maier, Solid State Ionics 175 (2004) 7.
[30] M. Han, X. Tang, H. Yin, S. Peng, J. Power Sources 165 (2007) 757–763.